International Journal on Recent and Innovation Trends in Computing and Communication
ISSN: 2321-8169 Volume: 11 Issue: 4
DOI: https://doi.org/10.17762/ijritcc.v11i4.6446
***Article Received**: 10 February 2023 **Revised**: 08 March 2023 **Accepted**: 19 March 2023*

An Automated Abnormality Diagnosis and Classification in Brain MRI using Deep Learning

***Ravendra Singh[1], Bharat Bhushan Agarwal[2]**
[1]Department of CSE, IFTM University, Moradabad, India
ravendra85@gmail.com
[2]Deparment of CSE, IFTM University, Moradabad,India
bharatagarwal9@gmail.com

Abstract— A technique for recognising and labeling malignant brain tissues according to the types of tumours present is known as tumour classification. Magnetic resonance imaging (MRI) can be used in clinical settings to both diagnose and treat gliomas. For clinical diagnosis and treatment planning, the ability to correctly diagnose a brain tumour from MRI images is essential. Manual classification, however, is not feasible in a timely manner due to the enormous volume of data produced by MRI. For classification and segmentation, it is required to employ automated algorithms. However, the numerous spatial and anatomical differences present in brain tumours make MRI image segmentation challenging. We have created a unique CNN architecture for classifying three different types of brain cancers. The new network was demonstrated to be more straightforward than earlier networks using MRI images with contrast-enhanced T1 pictures. Two 10-fold cross-validation techniques, two datasets, and an evaluation of the network's performance were used. A piece of upgraded picture information is used to assess the transferability of the network as part of the subject-cross-validation process. When used for record-wise cross-validation, this method of tenfold cross-validation ground set has an accuracy rate of 92.65 percent. Radiologists who operate in the ground of medical diagnostics may find the newly proposed CNN architecture to be a helpful decision-support tool due to its new transferability capability and speedy execution..

Keywords- Computer-aided diagnosis, Convolutional neural network, Brain tumor detection systems, Classification.

I. INTRODUCTION

A secondary tumour is a collection of cancer cells that have spread from another organ of the body. A primary tumour is a tumour that develops in the brain and does not spread to other organs. A brain tumour is a serious problem in today's healthcare system that could result in the patient's demise. Early identification can reduce the risk of developing cancer, although this is not always the case. A tumour can be benign, pre-carcinogenic, or malignant, in contrast to cancer. Most benign tumours can be resected and do not transmit to other tissues or organs, in contrast to malignant tumours [2]. Gliomas, meningiomas, and tumours of the hypothalamus are some of them.

The most frequent benign tumour of the three is a meningioma, and the most frequent malignant tumour is a glioma. It's important to keep in mind that pituitary tumours, despite being benign, can nevertheless have negative impacts on health [4]. A critical step in clinical laboratories and the consequent successful evaluation of patients is the right separation between these three types of cancer. This will allow for the accurate identification of these tumours.

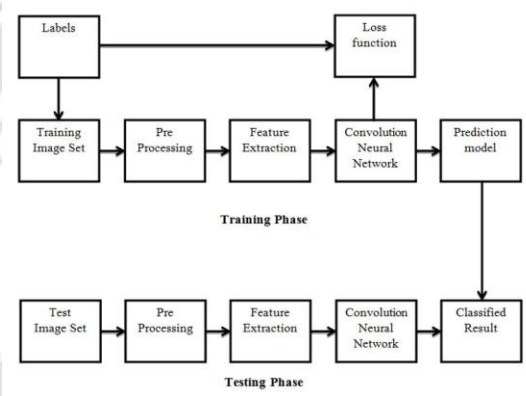

Figure 1. Tumor classification method using CNN

Brain tumours can be accurately diagnosed using magnetic resonance imaging, but this technique's full potential is constrained by the enormous amount of data that image collection equipment produces [5]. Throughout the image acquisition process, various excitation and repetition lengths result in various MRI modalities. Only with the use of distinct MRI modalities, which provide multiple types of tissue contrast pictures, can the architecture of a tumour be accurately segmented and recognised. Additionally, T1-weighting is used in T1-Gd, T1-W, and T2-weighted MRIs [6]. After a fluid attenuated inversion, recovery. In CT images, abscess sites can be distinguished from healthy tissues by a strong T2 signal. T1-

International Journal on Recent and Innovation Trends in Computing and Communication
ISSN: 2321-8169 Volume: 11 Issue: 4
DOI: https://doi.org/10.17762/ijritcc.v11i4.6446
***Article Received**: 10 February 2023 **Revised**: 08 March 2023 **Accepted**: 19 March 2023*

Gd pictures can reveal the brilliant side of the accumulating gadolinium ions. Since this signal of the hydrogen atoms in that solution is reduced, FLAIR images can be utilised to distinguish from edoema and that liquid. Isolating the disease from the equilibrium of healthy brain cells is one of the toughest parts to do in these circumstances in order for any treatment can be administered without damaging the best tissues while removing the terrible people.

It is essential to precisely distinguish the tumour first from adjacent dopaminergic neurons in order to prevent a mistaken prognosis that could endanger the treatment regimen. Individuals with brain tumours who had MRIs showed a wide variety of tumour sizes, forms, and placements.. The boundaries of the tumour are murky and inconsistent in several ways. As a result, defining the precise tumour borders and minimising error are very challenging undertakings. To recognise and categorise Region of interest using various neural networks, a sizable number of pictures must be handled in the database. Likewise, because MRI scans can be conducted in a range of dimensions, it is possible to increase the database by using every plane that is available. Overfitting may exacerbate Convolutional neural networks are known to require pre-processing and feature engineering. The main objective of this study is to categorise 3 distinct tumour kinds in an uneven database using a CNN. This database is commonly utilised in artificial intelligence research and is tiny in size compared to other MRI image collections. We set out to demonstrate that smaller architectures can perform on par with bigger ones. The costs of implementation and training are lower when switching to a less complex network. This is a serious problem because, due to a lack of assets, the system is challenging to utilise for cancer laboratories and on platforms. In principle, a system should be beneficial when utilised for routine clinical diagnosis. We sought to determine whether subject-wise pass may improve the network's capacity for generalisation during drug testing. In this work gliomas, pituitary, and meningiomas tumours- each of which was visible on T1 -MRI images that are weighted for contrast are classified using a novel form of CNN. Accuracy scores and confusion matrices are used to present the results. It is also demonstrated how this tactic stacks up against the state of the art at the time.

The remaining text is split into four separate sections and is organised alphabetically. We'll discuss typical MR image formats and the significance of contrast settings in Section 2 of this article. The broad framework that governs how methods for identifying brain tumours work is briefly covered in Section 3. The most well-known datasets in this field are also highlighted. Section 4 contains the discussion and conclusions. Section 5 concludes with a summary of the issues and solutions for the future.

II. LITERATURE SURVEY

The essential initiatives for classifying and segmenting brain tumours using MR images are briefly covered in this section. Clustering algorithm [7], unsupervised forests [8, choice of forests [9], analysis of principal components [10], and fuzzy random forests were some of the first machine learning techniques created and support vector machines [7]. These algorithms frequently classify image voxels using hand-crafted features, which calls to select the most interesting traits from training photos, a human specialist is needed. Recently, encouraging results have been obtained when segmenting medical pictures using DL-based techniques [11]. Since DL techniques can routinely learn complicated picture features from the training data, they enable us to create feature vectors that are more reliable. A variety of DL models have been developed for robotic tumour identification with positive outcomes [12]. Pereira and associates constructed two distinct 2D CNNs with higher sections as a clustering classifier in order to isolate both LG and HG glioblastomas. The [13] 2D CNN method, which integrates global and local information on large patches, offers two choices. For instance, a local approach examines information in the immediate area, whereas a major approach examines the wider context of MRI. A densely integrated CRF network was used in the comment step by [14] to analyse 3D patches, two feeds, and globally relevant data. Tumor division can be improved by utilising another more powerful version of DeepMedic that captures residual connections [15]. The aforementioned methods developed using CNNs for brain tumour classification take into account local areas in MRI images to categorise each patch of a brain tumour [16]. The centre pixel is labelled in accordance with the classification results; as a result, it only looks into spatially constrained contextual data.

Devastating natural and medical picture separation using FCNNs has produced positive outcomes. kernels for compression are used in the FCNN in place of completely linked layers. The image is scaled using layers of upsampling and deconvolution to its original size. Due to its extensive training, the model outperforms patch-level categorization techniques. In the incoming cascade CNN design, the second layer receives extra input in the form of pixel-wise prediction from the first CNN which the author first described in [17]. A two-stage training strategy with a multi-cascaded network is utilised to balance out an unbalanced label distribution[18]. Developed a comprehensive reporting structure for the outcomes of tumour segmentation using FCNN and CRFs. [19] indicated that in order to account for both the effective feature multi-scale properties of 3D MRI images, a non - linear and non convolutional network should be used as well as the local pixel dependencies. In order to further enhance the outcomes, CRFs are employed to soften

International Journal on Recent and Innovation Trends in Computing and Communication
ISSN: 2321-8169 Volume: 11 Issue: 4
DOI: https://doi.org/10.17762/ijritcc.v11i4.6446
***Article Received**: 10 February 2023 **Revised**: 08 March 2023 **Accepted**: 19 March 2023*

the edges of the tumour and lower false positives. U-Net is a compression algorithm adaptation that starts with a regular FCNN and employs downsampling at each layer to record relevant data and data augmentation at each layer to enhance the image size and permit fine localized and identification[20]. Modified the U-net CNN [21] architecture for tumour segmentation. By integrating dice-based loss functions with data augmentation, they increased segmentation accuracy. The watershed segmentation technique was used to divide up a brain tumour [22]. They employed cheap, manually created feature maps to build the KNN classifier. The overall accuracy they were able to achieve was 86%. An transceiver architecture was used to distinguish target tissue from proper brain regions in [23]. Through using SegNet design, a depth-four generator, and VGG16, this method achieves local features with non-linear up averaging. Without using any post-processing, this method produced an average dice score of 0.931. An encoder with a fully linked decoder rather than a deconvolutional decoder was recommended for FR-MRINet [24]. Using the local cleaning approach, anomaly zones—or non-tumor areas—that are predicted to become tumours are cleaned. Neural networks employ fourier filters in each teaching layer to maintain the complexity of the network and enhance the network's understanding of the input data. The 11-layer block mentioned in [25] included five activation functions with 3x3 filters, highest total layers, and three fully connected layers. Using the mean and standard deviations of the training images, the authors calculated the average and standard deviation for each training image. This was carried out to guarantee that the intensity of all images was the same prior to training. It has a frequency of 88% for the whole tumour, 83% for the central tumour, and 77% for the aggressive tumour in the BraTS dataset. It was suggested that brain tumours in inter MRI images might be automatically segmented using a specific tri convolution neural network in [26]. The processing time is lengthy, but 3D visualisation gives radiologists a greater understanding of the tumor's development. ReLU, batch normalising layers, 3D max-pooling layers, and the 3x3x3 convolution filter all combine to make the feature map smaller. The length, width, channels, and patterns of the three-dimensional images are piled up into a four-dimensional volume, or 4D volume. For the overall tumour and the core tumour, the BraTS dataset yielded results of 87, 77, and 73 percent, respectively. It has been demonstrated that convolutional networks are capable of performing both object identification and categorization [27]. The test image of a scene can be categorised using either the labeling of a solid body or the category of the entire input window. Instance separation [29], stereo-depth [28], posture assessment [28], and a host of other tasks have all been carried out using CNNs [30]. CNNs may be used in these research methodologies to either detect regional characteristics or generate descriptors of distinct proposal areas. Fully-Convolutional Network construction (FCN) has significantly improved segmentation [17]. Giving CNNs inputs of any magnitude is one of the best methods to help them progress. The proposed network performs remarkably well on the PASCAL VOC- 12 benchmark dataset. Many amazing improvements have been made to CNNs' general effectiveness and performance. By expanding the conventional LeNet, this idea was initially used for digit string recognition [27]. From one-dimensional input strings, [28] were able to get results using Viterbi decoding techniques. Later, by creating a new two-dimensional map model for CNN outputs, [29] improved this strategy. This method was used to identify a postal address block's four corners. These revolutionary developments in FCN will support future advances in CNNs for detection [30] showed a CNN segmentation based on inferred FCN for C-Elegans tissues. The author of [31] suggested a network that makes use of a Conditional Random Field with full connectivity to predict labels pixel-by-pixel and improve the label map. The random forest-based classifiers and FCN 2.0 are two of the most recent advances ([32]). Recent advances in fast convolutional neural networks (FCNs) and pixel segmentation have substantially enhanced the object detection in a whole image. Multi-scale superpixels can be categorised into predefined groups using semantic segmentation techniques like those described in [33]. These investigations have also included the integration of pixel-wise labelling. Several techniques [34] identify region suggestions for absolute segmentation and improve labels in the image-level segmentation map. SfM surfacing [37] and object recognition in semantic pixel-wise categorization[36] are used in the road scene interpretation test CamVid [35]. To enhance the performance of the network, the per-pixel disturbance estimates were flattened by CRF. made by the classifier [38].

1. Dataset description and Methodology

With the aid of MRI imaging of brain tumours, this project aims to mix the advantages of well-liked deep CNN models for the automatic classification of tumours. It is anticipated that hybrid models will have higher classification accuracy. These sections provide a comprehensive description of the proposed hybrid architecture. The proposed strategy is demonstrated in Figure 3. Preprocessing, CNN there are three major types of post-processing: categorization, processes in the procedure.

1.1. Image Database

The image library for this study was made up of 30640 Figshare's T1-weighted counterpoint MRI pictures. Since it was initially released in 2015, it has undergone a number of revisions. Glioma (14260 photos), pituitary tumour (9300 images), and meningioma (7080 images) [47]. Figure 2 depicts examples of various tumours in addition to different planes.

International Journal on Recent and Innovation Trends in Computing and Communication
ISSN: 2321-8169 Volume: 11 Issue: 4
DOI: https://doi.org/10.17762/ijritcc.v11i4.6446
***Article Received**: 10 February 2023 **Revised**: 08 March 2023 **Accepted**: 19 March 2023*

Each of the tumours is surrounded by a crimson border. The number of photos is different for each subject.

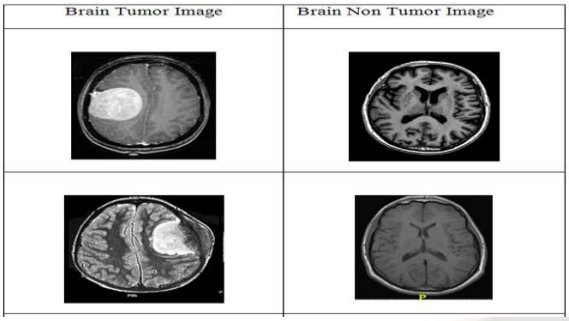

Figure 2. White shows the tumour in the pictures.

1.2. Pre-Processing

MRI spectroscopy is impacted by bias-induced field distortion. As an outcome, various tissues appear in the image at various intensities. It was fixed with N4ITK [6]. But it's likely that the dynamic range of a particular MRI sequence across a large number of people isn't always sufficient to correctly categorise a genetic makeup [37]. Furthermore, the same patient's scan pictures taken at different times or under different situations may show alterations [7, 38]. Due to this, we used [39] intensity normalisation to improve consistency between patients and acquisitions by adjusting the contrast and intensity range. A training set is used to establish the percentile strength for each standardized episode, and this percentile strength is subsequently selected for each MRI series. Following training, the sensitivities between two features are normalised by linearly converting the initial strengths into the respective learnt landmarks.It is simple to compare participant histograms once this is completed. The retrieved training patches for each sequence were first normalised, and then t The confidence interval and mean brightness were computed. For the region of each series, the range and mean are adjusted to 0 and 1, respectively. Testing patches are standardised by training patches' mean and standard deviation.

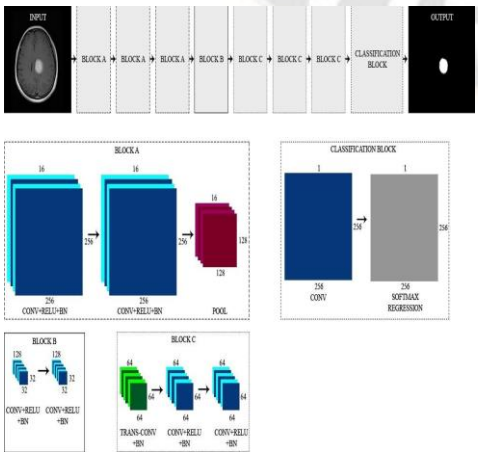

Figure 3. Proposed CNN architecture.

1.3. Training Network

Performance analysis of the network was done using K-fold pass. We performed tenfold cross-validation using two different methods. Each tumour type was recorded in one of the ten nearly equal pieces of data that were selected randomly, and each piece was then bridge record by record. Each of the ten equally sized data chunks was comprised of data from a specific person. This was the second way we processed the data. Thus, inter by the subject was used to ensure that each batch of data included information from two individuals independent of the type of tumour. Second, the tendency of the network to spread medical insights was evaluated. The ability to diagnose patients for whom no measurements were made during the course work is referred to as "overfitting competence" in clinical practitioners. The following approaches required two bits for testing, two more for confirmation, and two as much for training. All methods, both conventional and improved datasets.

1.4. Convolutional Neural Network

CNN has been applied to gather several ground-breaking insights and to win major competitions [7]. Deep networks [43, 44] mix a message or a picture with cores to produce saliency map. Each unit of the inversion layer is connected to the layer directly above by the density of the core. Relu is used to change the kernel intensities during retraining. Deep networks require fewer inputs to train than deep FC layers because all units inside the same feature extraction share the same kernels. This approach makes it possible to train CNN more fast and easily while minimising overfitting. Because the same kernel is used throughout the image, a feature can be recognised whether or not the image is translated. Kernels are a particularly valuable tool since they take into consideration contextual information from the surrounding area. Each brain unit's output is often subjected to a non-linear activation function. The more convolutional layers there are, the more abstract the retrieved characteristics become. For instance, edges are improved in the first layers before being combined as motifs, components, or objects in later layers [25]. CNN should be interested in the following subjects:

Initialization: Convergence is a critical goal. As an initialization method, the Xavier initialization is employed [41]. If activations and gradients aren't under control, back-propagated gradients might disappear or erupt.

Activation Function: It is in capable of doing non-linear transformations on the data. "ReLU" stands for "rectifier linear unit."

$$f(x) = \max(0, x) \qquad (1)$$

International Journal on Recent and Innovation Trends in Computing and Communication
ISSN: 2321-8169 Volume: 11 Issue: 4
DOI: https://doi.org/10.17762/ijritcc.v11i4.6446
***Article Received**: 10 February 2023 **Revised**: 08 March 2023 **Accepted**: 19 March 2023*

Improved training performance over the more traditional sigmoid or hyperbolic tangent functions and reduced training time [26, 42]. Imposing a constant 0 may, on the other hand, impede gradient flow and, as a result, the weights [43]. The LReLU (leaky rectifier linear unit) [43] inserts a tiny slope to the negative component of the function to overcome these constraints. In the simplest terms, this is defined as:

If x <0, f(x) = 0 and x >= 0, f(x) = x

$$f(x) = max(0, x) + \alpha\, min(0, x) \quad (2)$$

where is the leakyness parameter. In the last FC layer, we use Softmax.

Pooling: The feature maps combine features that are located close to one other. Small image modifications, such as trivial details, do not affect the representation because of this combination of potentially redundant characteristics; it also reduces the computing load of following steps. Max-pooling or average-pooling [25] are more commonly used to join features.

Regularization: Reduces overfitting. There are Dropouts in the FC layers [44, 45]. It randomly eliminates nodes from the network throughout each training stage. As a result, nodes in the FC levels are forced to improve their representations of the data, which prevents them from adapting to one another. All nodes are used during testing. For example, dropout may be considered as a bagging technique since each network is trained with only a fraction of the training data.

Data Augmentation: Overfitting may be reduced by using it to increase training sets. We limited the data augmentation to rotational operations because the patch's class is determined by the centre voxel. However, for segmentation, this might lead to incorrectly classifying the patch because some writers additionally take into account image translations [26]. As a result, during training, we expanded our data set by creating additional patches by rotating the original patch. The angle multiple of 90 was employed in our proposal, however, a different angle will be evaluated.

III. RESULTS AND DISCUSSION

The proposed CNN observations are illustrated using confusion vectors and are presented in Table 1 and shown in Fig 4.3 and 5. The outcomes of the recommended CNN are displayed in Figures 4 and 5. Confusion vectors' non-white rows and columns match to actual classes. Laterally presented are the proportions and numbers of correctly identified photographs. Sensitivity and specificity are shown in the final row and column, correspondingly. The total accuracy is displayed in the camera's lower right corner. The larger number reflects the number of images for each non-white box, while the smaller number shows the percentage of the class materials used for instruction and testing. The overall mean recall, reliability, and F1-score to ignore the mismatch of tumour classes are also included in Table 2 in the database.

Table 1. A Cross-validation test and 1-test employing two distinct cross-validation techniques

Approach	Accuracy(%)	Precision(%)	Recall (%)	F-Score(%)
10-fold-cross-validation	97.30	96.01	96.07	96.82
One test	96.29	97.04	97.86	97.22
10-fold-cross-validation	96.06	96.09	95.01	96.01
One test	97.01	97.85	96.72	96.87
10-fold-cross-validation	88.45	85.50	83.52	82.86
One test	92.29	89.47	85.44	83.51
10-fold-cross-validation	88.48	88.18	87.22	89.77
One test	92.44	83.54	84.57	83.78

Data from the original dataset were tested using a record-wise 10-fold cross-validation approach, as shown in Figure 4. The classification error after cross-validation is 4.6%.

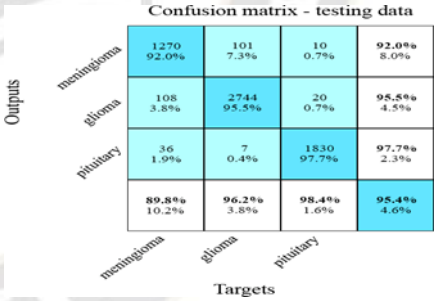

Figure 4. Records-wise 10-fold cross-validation with confusion matrices is used to validate the original dataset.

The tenfold cross-validation method shown in Figure 5 was used to subject-wise validate the data from the original dataset. The testing set's categorization error is 15.7 percent. Because the projections were made using formerly unobserved data, the network's quality is poorer than that achieved using career-high cross-validation because the predictions were produced using previously unobserved data.

International Journal on Recent and Innovation Trends in Computing and Communication
ISSN: 2321-8169 Volume: 11 Issue: 4
DOI: https://doi.org/10.17762/ijritcc.v11i4.6446
***Article Received**: 10 February 2023 **Revised**: 08 March 2023 **Accepted**: 19 March 2023*

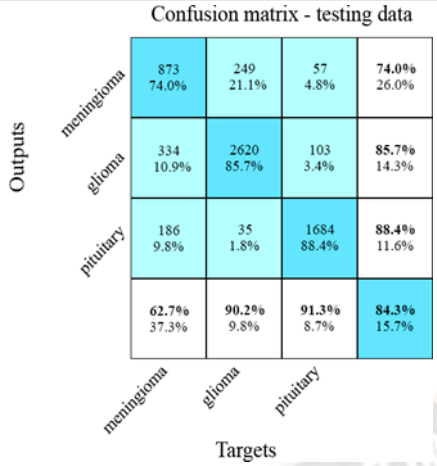

Figure 5. The testing data's subject-wise ten-fold cross-validation and confusion matrices for the original dataset are displayed.

The categorization error rate for test data is 11.5%. However, because the data collection is not very massive, the suggested CNN design performs better when more data is supplied. However, though with a wide range of data and more photographs for some patients, the findings are not as accurate as they'd be if we had used record-wise cross-validation. Since the data was segmented, increasing the victim count has taken on greater significance. Because of its lack of specificity and sensitivity, lesion tumour monitoring was the most challenging. This may be the case because, due to their position and physical attributes, hemangiomas are the most challenging of the three tumours to recognise. Graphics rendering typically takes less than 20 milliseconds, which is quite good.

Figure 6 shows gliomas (left), meningiomas (middle), and a pituitary tumour (right) (right).

On these photos, tumour categorization is shown. They are distinguished by three distinct colours: red for the anticipated tumour position, green for the actual tumour location, and yellow for the overlap between those two areas.

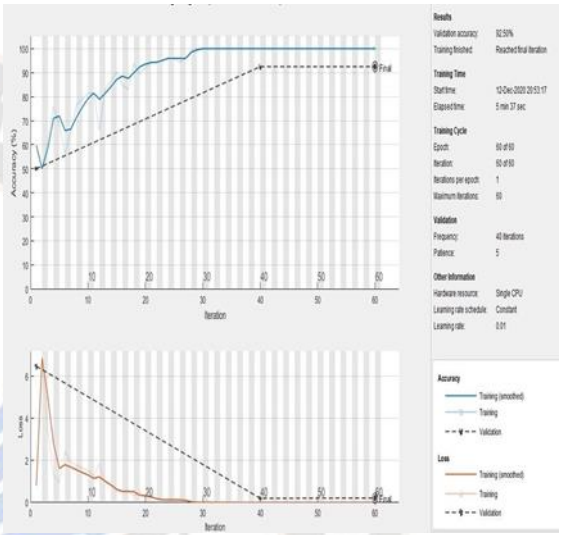

Figure 7. Performance assessment of the suggested CNN model.

Table 2. Various network topologies that have been trained and tested using the augmented dataset.

Methods	Data Division	Accuracy(%)	Precision(%)	Recall(%)	F1-Score(%)
Proposedmethod	60% of the data is in the training sets, 20% is in the validation sets, and 20% is in the test sets.	97.17	97.15	97.82	97.44
KNN-Classifier	70% of the data is present in the training sets, but only 30% is present in the validation and test sets.	88.53	88.16	87.77	85
SVM-GRB Classifier	30% of the data is in the validation and test sets, whereas 70% is in the training sets.	90. 01	89.05	88.74	87

It is quicker to build a network using simply Using a delineation technology or a qualified specialist to mark the data will demand the region of interest or another segregated component. the segmented portions.

IV. CONCLUSION AND FUTURE SCOPE

A cutting-edge CNN structure is created in this work to categorise brain tumours. The 3 separate tumour types were distinguished using a database of Diffusion - weighted contrast-enhanced MRI scans. Our neural network is easier to instal and can be controlled on modern desktop computers. Since we used entire photos as input, there was no need for any preprocessing or tumour division. The procedure's low resource needs throughout both development and production make this possible. Local networks are crucial since the technique can be used to mobile devices for diagnosis in underdeveloped nations [48]. Additionally, the network transmits each image in about 20 milliseconds. We evaluated the system using 10-fold bridge on both the basic and enhanced picture sets. Generalization in clinical diagnosis

International Journal on Recent and Innovation Trends in Computing and Communication
ISSN: 2321-8169 Volume: 11 Issue: 4
DOI: https://doi.org/10.17762/ijritcc.v11i4.6446
Article Received: 10 February 2023 Revised: 08 March 2023 Accepted: 19 March 2023

necessitates making assumptions about people for that we have no information. Thus, there shouldn't be any observations from people in the testing phase in the test set. If this need is not met, intricate variables may exhibit an unreasonable high level of precision because of the unclear link between a patient's identification and diagnosis. We are committed to topic discharge as an outcome of the data. In the coming, we'll assess our neural network's ability on additional medical images to see if it can be improved.

REFERENCE

[1] Murthy, M. Y. B., Koteswararao, A., & Babu, M. S. (2022). Adaptive fuzzy deformable fusion and optimized CNN with ensemble classification for automated brain tumor diagnosis. *Biomedical engineering letters*, *12*(1), 37-58.

[2] Gurunathan, A., & Krishnan, B. (2022). A Hybrid CNN-GLCM Classifier For Detection And Grade Classification Of Brain Tumor. *Brain Imaging and Behavior*, 1-18.

[3] Ak, A., Topuz, V., & Midi, I. (2022). Motor imagery EEG signal classification using image processing technique over GoogLeNet deep learning algorithm for controlling the robot manipulator. Biomedical Signal Processing and Control, 72, 103295.

[4] Khan, A. R., Khan, S., Harouni, M., Abbasi, R., Iqbal, S., & Mehmood, Z. (2021). Brain tumor segmentation using K-means clustering and deep learning with synthetic data augmentation for classification. Microscopy Research and Technique, 84(7), 1389-1399.

[5] Bhuvaneswary, N., Lakshmi, A., Bhuvaneswari, E., Ahmed, P. J., & Vaishnavi, M. (2022, March). Multi Modal Image Fusion Technique For Detecting Brain Tumor. In 2022 6th International Conference on Computing Methodologies and Communication (ICCMC) (pp. 1364-1371). IEEE.

[6] Singh, R., & Agarwal, B. B. (2022). Abnormality detection and classification from brain MRI using machine learning. International Journal of Health Sciences, 6(S3), 9170–9180. https://doi.org/10.53730/ijhs.v6nS3.8242.

[7] Amin, J., Sharif, M., Raza, M., & Yasmin, M. (2018). Detection of brain tumor based on features fusion and machine learning. Journal of Ambient Intelligence and Humanized Computing, 1-17.

[8] Usman, K., & Rajpoot, K. (2017). Brain tumor classification from multi-modality MRI using wavelets and machine learning. Pattern Analysis and Applications, 20(3), 871-881.

[9] Pereira, S., Meier, R., Alves, V., Reyes, M., & Silva, C. A. (2018). Automatic brain tumor grading from MRI data using convolutional neural networks and quality assessment. In Understanding and interpreting machine learning in medical image computing applications (pp. 106-114). Springer, Cham.

[10] Farhi, L., Zia, R., & Ali, Z. A. (2018). 5 Performance Analysis of Machine Learning Classifiers for Brain Tumor MR Images. Sir Syed University Research Journal of Engineering & Technology, 8(1), 6-6.

[11] Vijh, S., Sharma, S., & Gaurav, P. (2020). Brain tumor segmentation using OTSU embedded adaptive particle swarm optimization method and convolutional neural network. In Data visualization and knowledge engineering (pp. 171-194). springer, Cham.

[12] Mohsen, H., El-Dahshan, E. S. A., El-Horbaty, E. S. M., & Salem, A. B. M. (2018). Classification using deep learning neural networks for brain tumors. Future Computing and Informatics Journal, 3(1), 68-71.

[13] Veeraraghavan, A., Roy-Chowdhury, A. K., & Chellappa, R. (2005). Matching shape sequences in video with applications in human movement analysis. IEEE Transactions on Pattern Analysis and Machine Intelligence, 27(12), 1896-1909.

[14] Litjens, G., Kooi, T., Bejnordi, B. E., Setio, A. A. A., Ciompi, F., Ghafoorian, M., ... & Sánchez, C. I. (2017). A survey on deep learning in medical image analysis. Medical image analysis, 42, 60-88.

[15] Akkus, Z., Galimzianova, A., Hoogi, A., Rubin, D. L., & Erickson, B. J. (2017). Deep learning for brain MRI segmentation: state of the art and future directions. Journal of digital imaging, 30(4), 449-459.

[16] Cheng, J., Huang, W., Cao, S., Yang, R., Yang, W., Yun, Z., ... & Feng, Q. (2015). Enhanced performance of brain tumor classification via tumor region augmentation and partition. PloS one, 10(10), e0140381.

[17] Ma, X., Liu, W., Tao, D., & Zhou, Y. (2019). Ensemble p-laplacian regularization for scene image recognition. Cognitive Computation, 11(6), 841-854.

[18] Ramirez-Quintana, J. A., Madrid-Herrera, L., Chacon-Murguia, M. I., & Corral-Martinez, L. F. (2021). Brain-computer interface system based on p300 processing with convolutional neural network, novel speller, and low number of electrodes. Cognitive Computation, 13(1), 108-124.

[19] Roy, Y., Banville, H., Albuquerque, I., Gramfort, A., Falk, T. H., & Faubert, J. (2019). Deep learning-based electroencephalography analysis: a systematic review. Journal of neural engineering, 16(5), 051001.

[20] Jiang, X., Gu, X., Xu, K., Ren, H., & Chen, W. (2019). Independent decision path fusion for bimodal asynchronous brain–computer interface to discriminate multiclass mental states. IEEE Access, 7, 165303-165317.

[21] Mohanty, R., Sinha, A. M., Remsik, A. B., Dodd, K. C., Young, B. M., Jacobson, T., ... & Prabhakaran, V. (2018). Machine learning classification to identify the stage of brain-computer interface therapy for stroke rehabilitation using functional connectivity. Frontiers in neuroscience, 12, 353.

[22] Bablani, A., Edla, D. R., Tripathi, D., & Cheruku, R. (2019). Survey on brain-computer interface: An emerging computational intelligence paradigm. ACM Computing Surveys (CSUR), 52(1), 1-32.

[23] Chakladar, D. D., & Chakraborty, S. (2019). Feature extraction and classification in brain-computer interfacing: Future research issues and challenges. In Natural Computing for Unsupervised

Learning (pp. 101-131). Springer, Cham.

[24] Ieracitano, C., Mammone, N., Hussain, A., & Morabito, F. C. (2020). A novel multi-modal machine learning based approach for automatic classification of EEG recordings in dementia. Neural Networks, 123, 176-190.

[25] Kantak, S. S., Stinear, J. W., Buch, E. R., & Cohen, L. G. (2012). Rewiring the brain: potential role of the premotor cortex in motor control, learning, and recovery of function following brain injury. Neurorehabilitation and neural repair, 26(3), 282-292.

[26] Kasabov, N. K. (2014). NeuCube: A spiking neural network architecture for mapping, learning and understanding of spatio-temporal brain data. Neural Networks, 52, 62-76.

[27] Kasabov NK (2019) Time-space, spiking neural networks and brain-inspired artificial intelligence. Springer, Berlin

[28] Kingma DP, Ba J (2014) Adam: A method for stochastic optimization. arXiv preprint arXiv:1412.6980

[29] Krizhevsky A, Sutskever I, Hinton GE (2012) Imagenet classification with deep convolutional neural networks. In: Advances in neural information processing systems, pp 1097–1105.

[30] Chen X, Xie H (2020) A structural topic modeling-based bibliometric study of sentiment analysis literature. Cogn Comput 1–33

[31] Sultan, H. H., Salem, N. M., & Al-Atabany, W. (2019). Multi-classification of brain tumor images using deep neural network. IEEE Access, 7, 69215-69225.

[32] Roy, Y., Banville, H., Albuquerque, I., Gramfort, A., Falk, T. H., & Faubert, J. (2019). Deep learning-based electroencephalography analysis: a systematic review. Journal of neural engineering, 16(5), 051001.

[33] Bi, X., & Wang, H. (2019). Early Alzheimer's disease diagnosis based on EEG spectral images using deep learning. Neural Networks, 114, 119-135.

[34] Ullah, A., Anwar, S. M., Bilal, M., & Mehmood, R. M. (2020). Classification of arrhythmia by using deep learning with 2-D ECG spectral image representation. Remote Sensing, 12(10), 1685.

[35] Srinivasan, K., & Nandhitha, N. M. (2019). Development of Deep Learning algorithms for Brain Tumor classification using GLCM and Wavelet Packets. Caribb. J. Sci, 53, 1222-1228.

[36] Lakshmanaprabu, S. K., Mohanty, S. N., Shankar, K., Arunkumar, N., & Ramirez, G. (2019). Optimal deep learning model for classification of lung cancer on CT images. Future Generation Computer Systems, 92, 374-382.

[37] Kumar, P. R., Sarkar, A., Mohanty, S. N., & Kumar, P. P. (2020, October). Segmentation of white blood cells using image segmentation algorithms. In 2020 5th International Conference on Computing, Communication and Security (ICCCS) (pp. 1-4). IEEE.

[38] Singh, R., & Agarwal, B. B. (2022). A Hybrid Approach for Detection of Brain Tumor with Levy Flight Cuckoo Search. Webology, 19(1).

[39] Lakshmanaprabu, S. K., Mohanty, S. N., Krishnamoorthy, S., Uthayakumar, J., & Shankar, K. (2019). Online clinical decision support system using optimal deep neural networks. Applied Soft Computing, 81, 105487.

[40] Fernando, T., Denman, S., Ahmedt-Aristizabal, D., Sridharan, S., Laurens, K., Johnston, P., & Fookes, C. (2019). Neural memory plasticity for anomaly detection. arXiv preprint arXiv:1910.05448.

[41] Rehman, A., Naz, S., Razzak, M. I., Akram, F., & Imran, M. (2020). A deep learning-based framework for automatic brain tumors classification using transfer learning. Circuits, Systems, and Signal Processing, 39(2), 757-775.

[42] Tripathi, P. C., & Bag, S. (2020). Non-invasively grading of brain tumor through noise robust textural and intensity based features. In Computational intelligence in pattern recognition (pp. 531-539). Springer, Singapore.

[43] Mangla, M., Sayyad, A., & Mohanty, S. N. (2021, May). An AI and Computer Vision-based Face Mask Recognition & Detection System. In 2021 2nd International Conference on Secure Cyber Computing and Communications (ICSCCC) (pp. 170-174). IEEE.

[44] Kotia, J., Kotwal, A., & Bharti, R. (2019, October). Risk susceptibility of brain tumor classification to adversarial attacks. In International Conference on Man–Machine Interactions (pp. 181-187). Springer, Cham.

[45] Moccia, S., Foti, S., Routray, A., Prudente, F., Perin, A., Sekula, R. F., ... & Riviere, C. N. (2018). Toward improving safety in neurosurgery with an active handheld instrument. Annals of biomedical engineering, 46(10), 1450-1464.

[46] Singh, R., & Agarwal, B. B. (2022). An automated brain tumor classification in MR images using an enhanced convolutional neural network. International Journal of Information Technology, 1-10.

[47] Ipp.cbica.upenn.edu. 2022. Penn Imaging – Home. [online] Available at: <https://ipp.cbica.upenn.edu/> [Accessed 12 March 2022].

[48] Swati, Z. N. K., Zhao, Q., Kabir, M., Ali, F., Ali, Z., Ahmed, S., & Lu, J. (2019). Brain tumor classification for MR images using transfer learning and fine-tuning. Computerized Medical Imaging and Graphics, 75, 34-46.